Electronic Supplementary Information (ESI) for

Direct solvothermal phosphorization of nickel foam to fabricate integrated Ni_2P-nanorods/Ni electrodes for efficient electrocatalytic hydrogen evolution

Xiaoguang Wang, Yury V. Kolen'ko, Lifeng Liu*

International Iberian Nanotechnology Laboratory (INL), Av. Mestre Jose Veiga, 4715-330 Braga, Portugal

E-mail: lifeng.liu@inl.int

CONTENTS

1. Experimental Details

Fabrication of integrated Ni_2P-nanorods/Ni electrodes:

Nickel (Ni) foam was purchased from Heze Jiaotong Co. Ltd (110 PPI, 480 g m^{-2}, nominal thickness 0.3 mm). Before phosphorization, the Ni foam was cleaned in 6 M HCl (Sigma-Aldrich) by ultrasonication for 10 min, subsequently washed by water and acetone, and then dried at 50 °C for 10 min. Afterwards, around 0.2 g of Ni foam (ca. 2.4 × 2.4 cm piece) and 0.1 g of amorphous red phosphorous (Alfa Aesar, 98.9%) were loaded into a PTFE reaction cup (total volume 45 mL). 30 mL of anhydrous ethylenediamine (TCI, 98.0%) was then added into the reaction cup as a solvent. The PTFE cup was sealed by a PTFE cover, and fitted into a stainless steel autoclave. Subsequently, the autoclave was sealed, hand shaken and placed into a heating oven. The best results were achieved when the reaction was performed at 200 °C for 48 h under an autogenous pressure. The resultant foam sample was cleaned by 5 min ultrasonication in deionized (DI) water, then in ethanol, and finally in acetone. After solvothermal treatment, the originally shiny grey Ni foam turned to blackish and became quite brittle (**Figure S1**, inset). The original macroporous morphology, however, was preserved.

Structural characterization:

The morphology and microstructure of the as-prepared Ni_2P nanorods were characterized by scanning electron microscopy (SEM, Quanta 650 FEG, FEI) and aberration-corrected transmission electron microscopy (TEM, Titan ChemiSTEM 80-200, FEI, operating at 200 kV). The chemical composition of Ni_2P nanorods was analyzed by energy dispersive X-ray spectroscopy (EDX) in scanning TEM mode. For TEM investigation, the Ni_2P-nanorods/Ni was pulverized and dispersed in isopropanol (Sigma, 99%) by ultrasonication. A drop of suspension was then placed on a carbon-coated copper grid. The grid was subsequently dried at 110 °C in a vacuum oven for 1 h.

Powder X-ray diffraction (XRD) analysis was carried out on a X'Pert PRO diffractometer (PANalytical) set at 45 kV and 40 mA with Cu *K*α radiation (λ = 1.541874 Å) and a PIXcel detector. Data were collected using Bragg-Brentano configuration in the 2θ range of 20°-80° with a scan speed of 0.01° s^{-1}. The XRD

patterns were indexed according to the International Centre for Diffraction Data (ICDD) PDF-4+ database. The phase composition analysis was carried out using HighScore software package (PANalytical).

Electrochemical Measurements:

All electrochemical measurements were conducted in a typical three-electrode cell with a N_2-saturated aqueous electrolyte of 0.5 M H_2SO_4 (pH = 0.28) using the as-prepared Ni_2P-nanorods/Ni foam as the working electrode, a graphite plate as the counter electrode, and a saturated calomel electrode (SCE) as the reference. For comparison, the electrocatalytic performance of a polished Pt foil (Alfa Aesar, 99.9%) and a bare Ni foam was tested under the same conditions as those used for the Ni_2P-nanorods/Ni electrode. Prior to the electrochemical measurement, the electrolyte was deaerated via bubbling of high-purity N_2 (99.999%) for 30 min, then maintaining the bubbling throughout the whole test to avoid any possible contribution from oxygen reduction. The electrochemical data were recorded using a Biologic VMP-3 potentiostat/galvanostat at room temperature (~ 25 ºC). Line sweep voltammetry (LSV) curves were measured at a sweep rate of 10 mV s^{-1}. The obtained LSV curves were corrected by the *iR* loss according to the following equation:

$$E_{corr} = E_{mea} - iR_s \qquad \text{(eq. S1)}$$

Where E_{corr} is the corrected potential, E_{mea} the measured potential and R_s the equivalent series resistance determined by electrochemical impedance spectroscopy (EIS). The accelerated degradation test (ADT) was conducted at a scan rate of 50 mV s^{-1} by performing cyclic voltammetry between -200 and 60 mV vs. RHE for 1000 continuous cycles. EIS measurements were carried out at different potentials in the frequency range of 10^5 to 0.05 Hz with a 10 mV sinusoidal perturbation. Unless otherwise specified, all potentials are reported versus reversible hydrogen electrode (RHE) by converting the potentials measured vs. SCE according to the following equation:

$$E\,(\text{RHE}) = E\,(\text{SCE}) + 0.241 + 0.059\,\text{pH} \qquad \text{(eq. S2)}$$

Supplementary Figures:

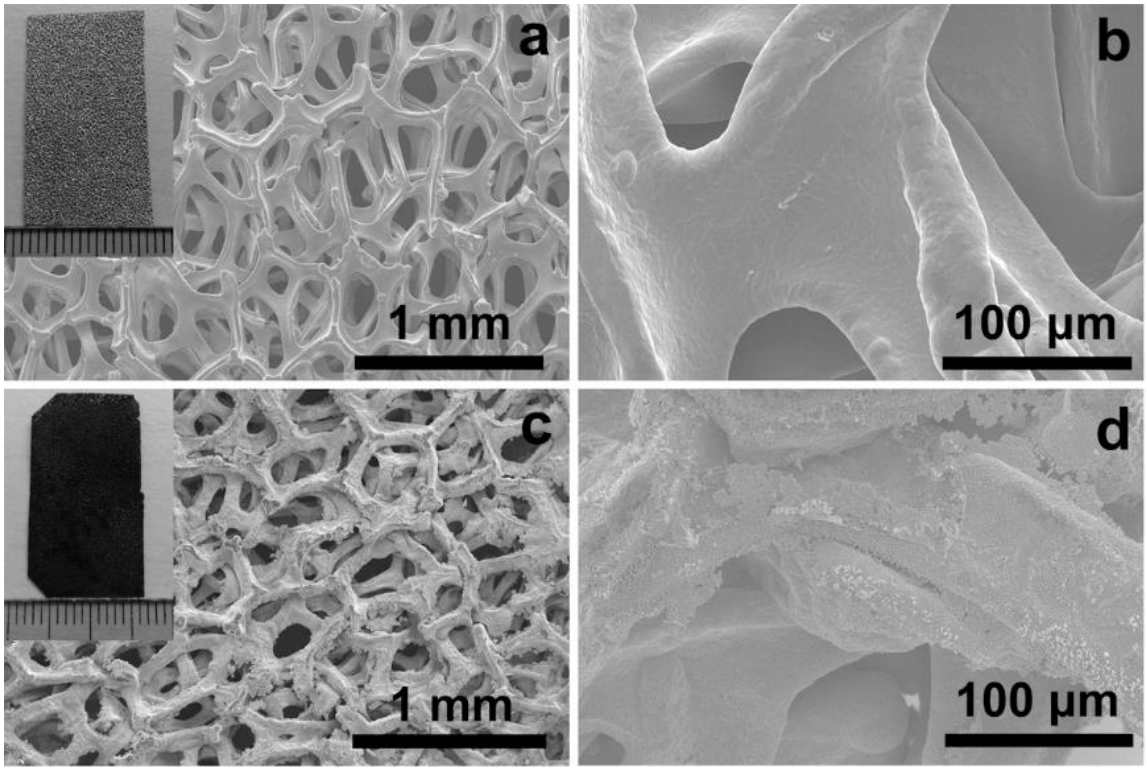

Fig. S1 SEM micrographs showing the morphology of a Ni foam (a, b) before and (c, d) after the phosphorization treatment under solvothermal conditions. The insets in (a) and (c) show the corresponding samples.

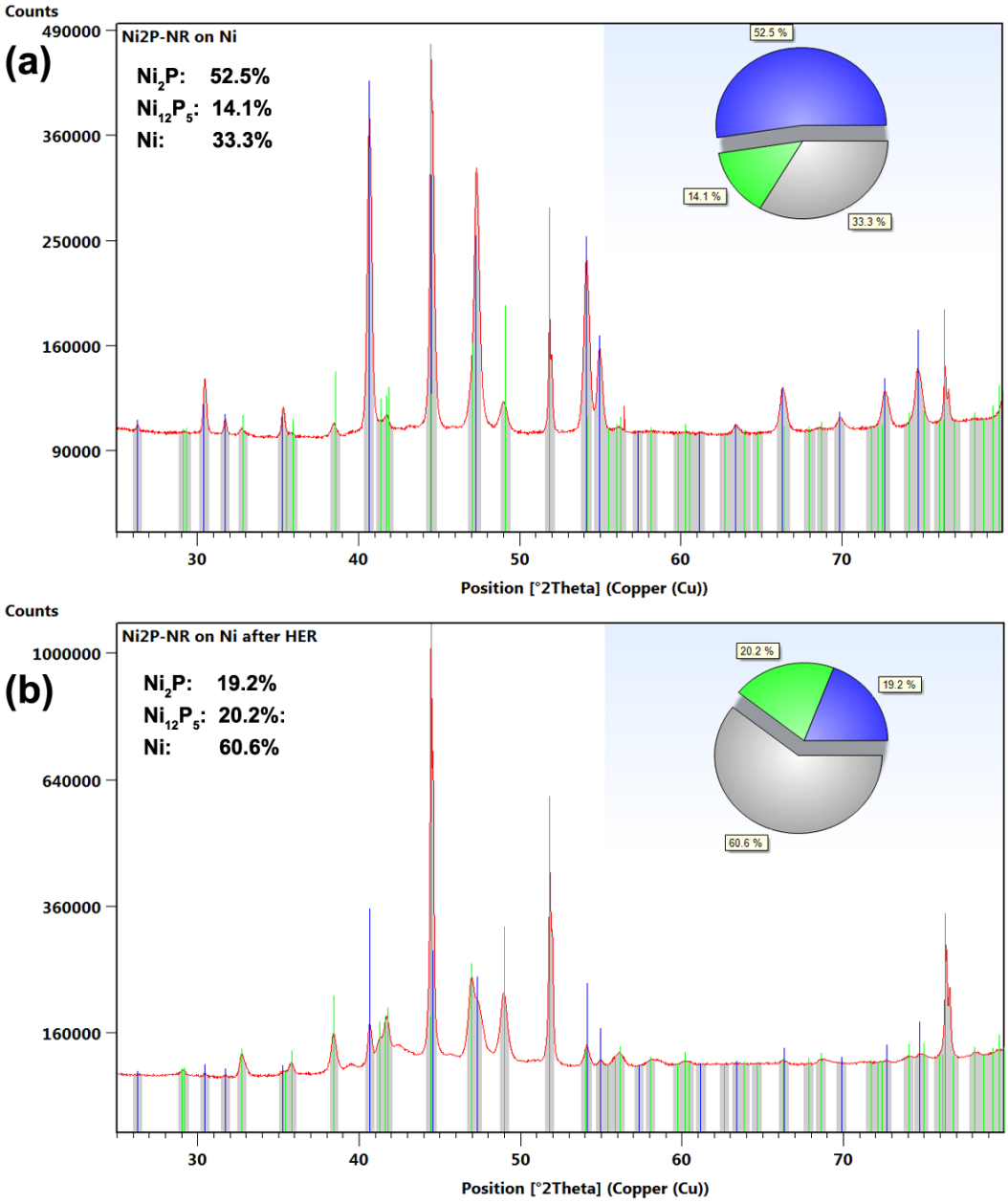

Fig. S2 Phase composition analysis of the Ni_2P-NRs/Ni composite electrode (a) before and (b) after the stability and durability tests.

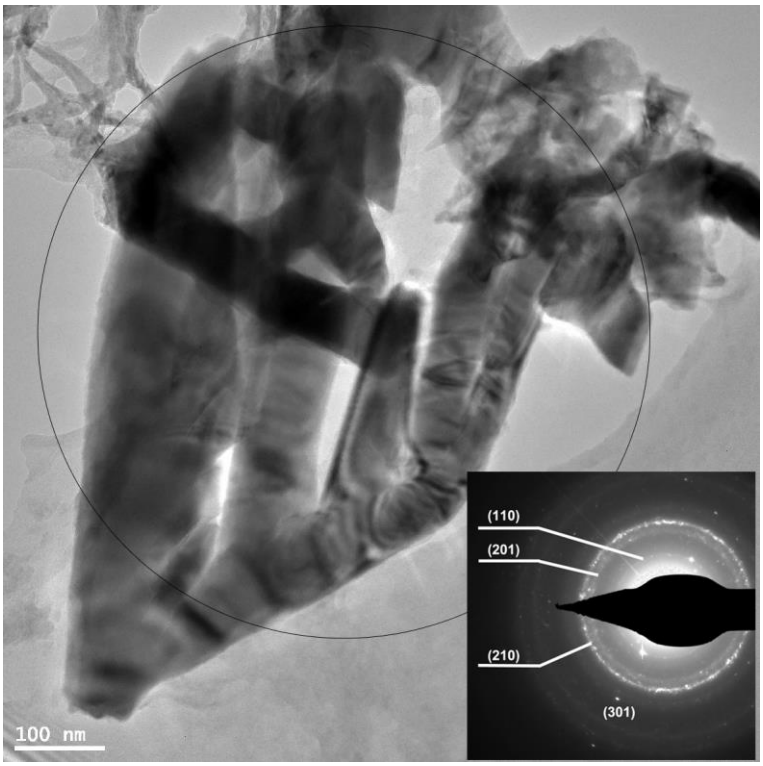

Fig. S3 Representative TEM image showing the morphology of the Ni_2P NRs. Inset: selected-area electron diffraction (SAED) pattern.

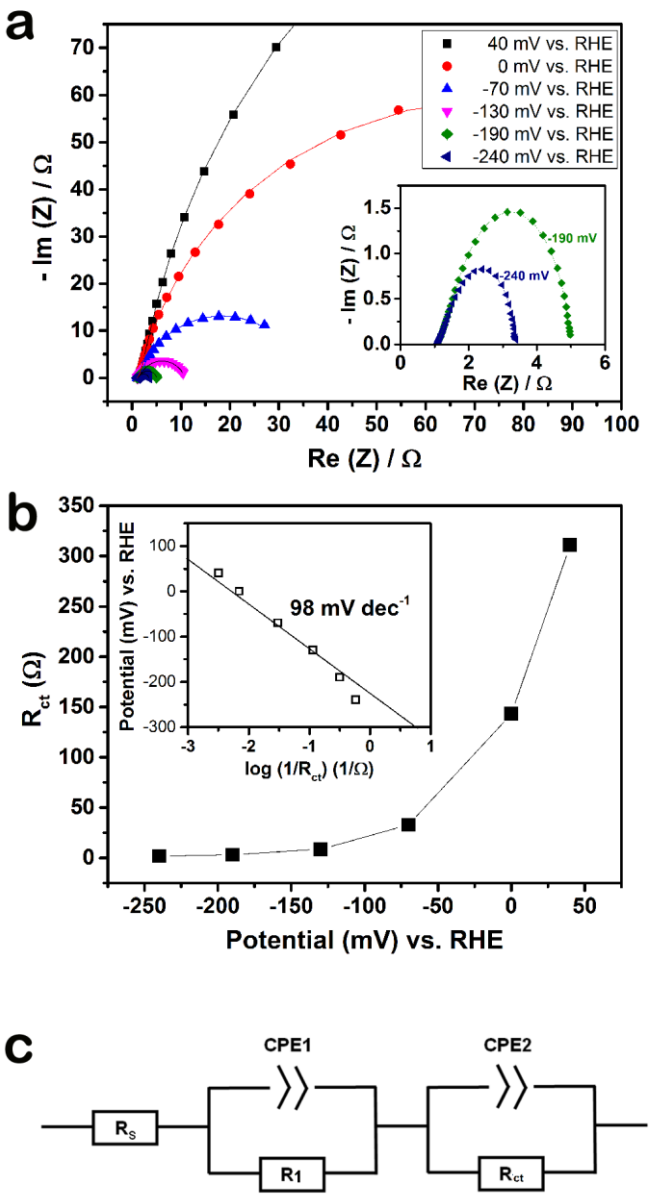

Fig. S4 (a) Nyquist plots of the Ni_2P-NRs/Ni electrode recorded at different applied overpotentials in the frequency range of 10^5 – 0.05 Hz. Symbols: experimental data; thin lines: fit curves. Inset: zoomed view of the plots measured at -190 and -240 mV. (b) The dependence of charge transfer resistance (R_{ct}) on the applied overpotentials. Inset: overpotential vs. log ($1/R_{ct}$). The symbols and thin line represent experimental data and their linear fit, respectively. (c) The equivalent circuit model used to fit the Nyquist plots shown in (a). R_s represents the equivalent series resistance, R_1 the electron/charge transport resistance in Ni_2P-NRs, and R_{ct} the charge transfer resistance at the electrode/electrolyte interface.

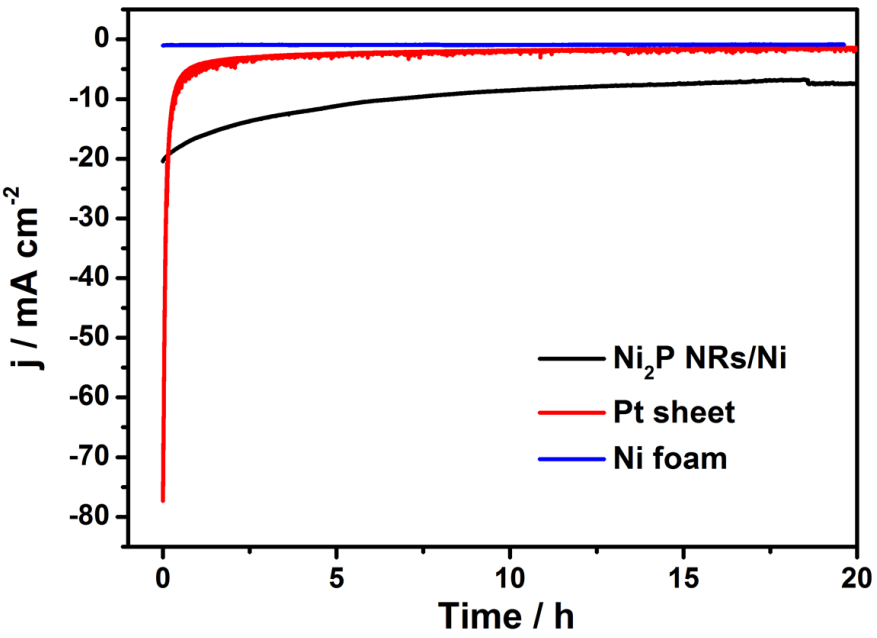

Fig. S5 Chronoamperometric profiles of Ni_2P-NRs/Ni composite electrode, bare Ni foam and Pt sheet, recorded at -200 mV vs. RHE in N_2-saturated 0.5 M H_2SO_4 solution.

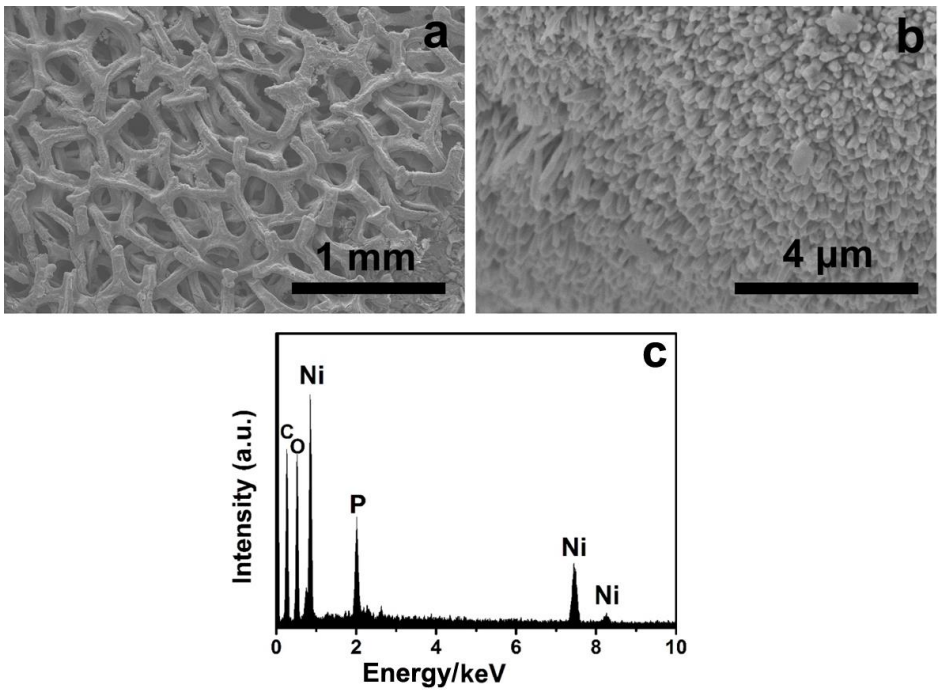

Fig. S6 (a) Low-, (b) high-magnification SEM images and (c) EDX spectrum of the Ni_2P-NRs/Ni electrode after accelerated degradation test for 1000 continuous cycles and subsequent chronoamperometric test at -200 mV for 20 h. It shows that the rod-like morphology virtually remains unchanged, but the content of O is dramatically increased in the tested electrode.

Supplementary Tables:

Table S1. Electrocatalytic performance of Ni_2P-NRs/Ni electrode in comparison with that of non-previous HER catalysts reported in the literature.

Catalyst	η_{10} **(mV vs. RHE)**	η_{20} **(mV vs. RHE)**	j_0 **(mA cm^{-2})**	**Reference**
MoS_2/RGO	-150	-176		[3b]
CoP	-226	-275	1.9×10^{-2}	[8b]
FeP nanosheets/GC	-240	-320		[9c]
MoP	-135	-167	3.4×10^{-2}	[11]
Bulk crystalline WP	-200	-223		[12]
Defect-rich MoS_2 nanosheets	-190	-214	8.91×10^{-3}	[S1]
WS_2 nanosheets	-233	-275		[6]
Bulk Mo_2C	-208	-224	1.3×10^{-3}	[15]
Bulk MoB	-212	-227	1.4×10^{-3}	[15]
Cu_3P NW/CF	-143	-157	1.8×10^{-1}	[10]
Cu_3P MP/CF	-200	-283	4.0×10^{-2}	[10]
Core-shell MoO_3-MoS_2	-255	-270	8.2×10^{-5}	[S2]
MoS_2@Au	-226		9.3×10^{-3}	[S3]
MoS_2 nanosheets/GC	-187	-210		[S4]
MoS_2/graphene/Ni foam	141	180		[S5]
$MoS_{2.7}$@NPG	-220	-245		[S6]
Ni_2P-NRsNi	**-131**	**-163**	**8.62×10^{-2}**	**This work**

Table S2. Comparison of electrocatalytic performance of the Ni_2P-NRs/Ni composite electrode with that of the nickel phosphide catalysts reported in the literature.

Catalyst	Electrolyte	Counter electrode	Onset potential (mV)	η_{10} (mV)	η_{20} (mV)	Tafel slope (mV dec^{-1})	j_0 (mA cm^{-2})	Reference
Ni_2P NPs on Ti	0.5 M H_2SO_4 solution	$RuIrO_x$/Ti mesh	45	90	130	46 (*η=25-125mV*) 81 (*η=150-200mV*)	3.3×10^{-2} (*η=25-125mV*) 4.9×10^{-1} (*η=150-200mV*)	[7a]
Ni_2P NPs/GC	1 M H_2SO_4 solution	Pt	50	120	140	87 (*η=60-140mV*)		[7b]
Ni_2P NPs/Ti	1 M H_2SO_4 solution	Graphite	60	120	138	60 (*η=70-150mV*)		[7c]
Ni_2P NRs/GC	0.5 M H_2SO_4 solution	Pt	60	265	330	112	5.1×10^{-2}	[7f]
Ni_2P NRs/Ti	0.5 M H_2SO_4 solution	Pt	150	500	650	144	3.7×10^{-2}	[7f]
Ni_2P NRs/Ti (annealed)	0.5 M H_2SO_4 solution	Pt	60	180	200	76	4.3×10^{-2}	[7f]
Ni_2P NCs/GC	0.5 M H_2SO_4 solution	Pt	62	137	180	49		[7d]
Ni_2P/C	0.5 M H_2SO_4 solution	Pt	60	87	115	54		[S7]
Ni_2P	0.5 M H_2SO_4 solution	Pt	125	225		86		[S7]
This work	**0.5 M H_2SO_4 solution**	**Graphite**	**33**	**131**	**163**	**106.1**	**8.62×10^{-2}**	

Table S3. Electrochemical impedance parameters obtained by fitting the Nyquist plots to the equivalent circuit model.

Potentials (mV)	**R_s (Ω)**	**R_1 (Ω)**	**Q_1 (F cm^{-2})**	**m_1**	**R_{ct} (Ω)**	**Q_2 (F cm^{-2})**	**m_2**
40	1.07	2.47	0.182	0.43	310.90	0.0148	0.92
0	**1.03**	**0.66**	**0.160**	**0.46**	**143.20**	**0.0199**	**0.87**
-70	1.07	0.91	0.123	0.47	32.90	0.0224	0.86
-130	1.07	1.02	0.129	0.46	8.68	0.0210	0.85
-190	1.08	0.78	0.0749	0.52	3.16	0.0170	0.90
-240	1.08	0.59	0.0635	0.54	1.73	0.0166	0.91

References:

[S1] J. Xie, H. Zhang, S. Li, R. Wang, X. Sun, M. Zhou, J. Zhou, X.W. Lou and Y. Xie, *Adv. Mater.*, 2013, **25**, 5807-5813.

[S2] Z. Chen, D. Cummins, B. N. Reinecke, E. Clark, M. K. Sunkara and T. F. Jaramillo, *Nano Lett.*, 2011, **11**, 4168-4175.

[S3] T. Y. Wang, L. Liu, Z. W. Zhu, P. Papakonstantinou, J. B. Hu and M. Li, *Energy Environ. Sci.*, 2013, **6**, 625-633.

[S4] M. A. Lukowski, A. S. Daniel, F. Meng, A. Forticaux, L. S. Li and S. Jin, *J. Am. Chem. Soc.*, 2013, **135**, 10274-10277.

[S5] Y. H. Chang, C. T. Lin, T. Y. Chen, C. L. Hsu, Y. S. Lee, W. J. Zhang, K. H. Wei and L. J. Li, *Adv. Mater.*, 2013, **25**, 756-760.

[S6] X. B. Ge, L. Y. Chen, L. Zhang, Y. R. Wen, A. Hirata and M. W. Chen, *Adv. Mater.*, 2014, **26**, 3100-3104.

[S7] Y. J. Bai, H. J. Zhang, X. Li, L. Liu, H. T. Xu, H. J. Qiu and Y. Wang, *Nanoscale*, 2015, **7**, 1446-1453.